This is a repository copy of *Structural interconnections and the role of heptagonal rings in endohedral trimetallic nitride template fullerenes.*.

White Rose Research Online URL for this paper:
http://eprints.whiterose.ac.uk/112116/

Version: Accepted Version

Structural interconnections and the role of heptagonal rings in endohedral trimetallic nitride template fullerenes

Li-Hua Gan*, Dan Lei and Patrick W Fowler*

School of Chemistry & Chemical Engineering, Southwest University, Chongqing, 400715 China

Department of Chemistry, Sheffield University, Sheffield, S3 7HF UK

E-mail: ganlh@swu.edu.cn (Gan); p.w.fowler@sheffield.ac.uk (Fowler)

Abstract: Recent experiments indicate that fullerene isomers outside the classical definition can also encapsulate metallic atoms or clusters to form endohedral metallofullerenes. Our systematic study using DFT calculations, suggests that many heptagon-including non-classical trimetallic nitride template fullerenes are similar in stability to their classical counterparts, and that conversion between low-energy non-classical and classical parent cages via Endo-Kroto insertion/extrusion of C_2 units and Stone-Wales isomerization may facilitate the formation of endohedral trimetallic nitride fullerenes. Close structural connections are found between favored isomers of trimetallic nitride template fullerenes from C_{78} to C_{82}. It appears that the lower symmetry and local deformations associated with introduction of a heptagonal ring favor encapsulation of intrinsically less symmetrical mixed metal nitride clusters.

Introduction

Endohedral metallofullerenes (EMFs) are compounds with metal atoms/clusters enclosed by a fullerene cage [1]. Since their early macroscopic synthesis [2], EMFs have attracted extensive interest from chemists, physicists and materials scientists [3]. To date, various EMFs have been characterized, in which metal atoms are included singly, in pairs, or in clusters [4]. Amongst the metallic cluster fullerenes, trimetallic nitride template fullerenes (TNT-EMFs) have attracted most interest owing to potential applications in electronics, optoelectronics and photovoltaics [5]. Given that all characterized bare fullerenes obeyed the isolated pentagon rule (IPR) [6] and that the first isolated EMFs had IPR parent cages, it was tacitly assumed by many researchers that the

parent cages of EMFs should also follow the IPR. This assumption was soon abandoned, as experiments suggested that electron transfer to the cage could stabilize an otherwise unstable parent cage [7]; Theoretical studies showed electron transfer from the metal atoms to the cage, and predicted that non-IPR EMFs could be favored over IPR EMFs in some cases [8]. Simplified models by us and others also suggested that the electron transfer would change the structural rules [9]. In 2000, EMFs $Sc_2@C_{66}$ and $Sc_3N@C_{68}$ [10] were synthesized. As neither C_{66} nor C_{68} can have IPR isomers, the reports of these two compounds clearly demonstrated that the set of possible parent cages of EMFs should be widened to include the family of classical fullerenes, i.e., both IPR and non-IPR cages. As the numbers of non-IPR isomers vastly exceed those of IPR isomers in the size range, and the chemical properties expected of IPR and non-IPR EMFs would be distinctly different, these two reports sparked a further wave of research on EMFs. From that point on, electron transfer was established as a crucial component of the model, with one role of the transferred electrons being stabilization of reactive pentalene motifs in non-IPR cages. Many non-IPR EMFs have since been reported [11-19]. This can be considered as the second stage of EMF science.

Interestingly, exohedral derivatives of fullerenes that contain heptagons, such as $C_{58}F_{18}$ [20], $C_{84}Cl_{32}$ [21], $C_{88}Cl_{22}$ [22] and $C_{96}Cl_{20}$ [23] have been obtained by chemical modification of classical fullerene molecules. Such work opens the way to chemical synthesis of further non-classical fullerene derivatives, but it deals with pre-formed fullerene cages and so does not give direct insight into the formation of either fullerenes or EMFs. Recently, however, the heptagon-including fullerene derivative $C_{68}Cl_6$ [24], and then the TNT-EMF

LaSc$_2$N@C$_{80}$, which includes a heptagonal face [25a], were synthesized in situ by the arc-discharge process. These reports demonstrate that heptagon-including fullerene-like molecules can form in a discharge, and once again lift a limitation on the likely candidates for parent cages of EMFs. As non-classical isomers greatly outnumber the classical fullerenes, these developments herald a third stage of EMF science.

However, as far as we know, no systematic study has been performed on non-classical EMFs to date. Meanwhile, the formation mechanisms of EMFs, including TNT-EMFs, remain unclear, even though nearly one hundred EMFs have been characterized [4]. In the present work, classical and non-classical TNT-EMFs of C$_{78}$, C$_{80}$ and C$_{82}$ were systematically studied with the help of an extended face-spiral algorithm for construction of candidates. The study shows that heptagon-including TNT-EMFs are close competitors of classical TNT-EMFs in terms of their energy and that there is a web of structural relationships between low-energy isomers of TNT-EMFs.

Computational Details

As the first step, we consider non-classical fullerenes with only one heptagonal face (f$_7$ = 1). A non-classical fullerene with a single heptagonal face contains f$_5$ = 13 pentagons and some hexagons, according to Euler's theorem [26]. Introduction of heptagonal faces tends to increase crowding of pentagons, and we consider here only those classical isomers (f$_5$ = 12) with at most three pentagon adjacencies, and those non-classical isomers (f$_5$ = 13) with at most two. Counts of the isomers by type and number of pentagon adjacencies are listed in the supporting information (S1). Topological coordinates [27] are used to provide initial cage structures, which are then optimized for charges 0, −2, −4 and −6 first using the semi-empirical PM3 level and then a selection of the best cages (60 for n = 78, 40 for n = 80, 30 for n = 82) at each charge, are optimized at the B3LYP/3-21G level using Gaussian 09 [28]. Based on the energy ranking for the optimized cages with charge -6, the favored cages are used as parents to construct Sc$_3$N, YSc$_2$N and LaSc$_2$N TNT-EMFs. Final optimisations are performed at the GGA-PW91 level with a double numerical basis set including d-polarization functions and a scalar relativistic correction, implemented in the Dmol^3 package [29]. The results are shown in Table 1 and Figure 1.
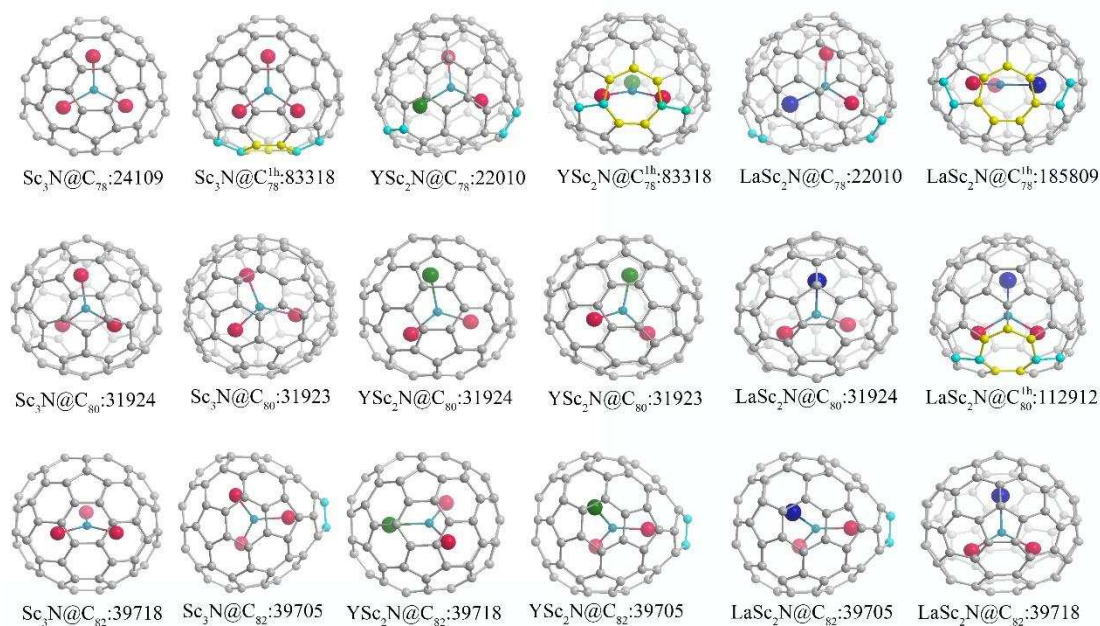

Fig. 1 Optimized structures of the two lowest-energy isomers for each MSc$_2$N@C$_n$ (M=Sc, Y and La, n=78, 80 and 82 at the GGA-PW91 level

Table 1 Low-energy isomers of TNT-EMFs. Numbers of pentagon adjacencies (N_{55}), relative energies (ΔE), HOMO-LUMO gaps (Δ_{HL}) and counterpoise-corrected encapsulation energies (E_{en}) of low-lying isomers of $MSc_2N@C_n$ (M=Sc, Y and La; n = 78, 80 and 82). Energies ΔE and E_{en} are given in kcal/mol, and gaps in eV.

Sc_3N					YSc_2N					$LaSc_2N$				
Cage	N_{55}	ΔE	Δ_{HL}	E_{en}	Cage	N_{55}	ΔE	Δ_{HL}	E_{en}	Cage	N_{55}	ΔE	Δ_{HL}	E_{en}
$C_{78:24109}$-D_{3h}	0	0.0	1.23	267.3	$C_{78:22010}$-C_2	2	0.0	1.37	313.7	$C_{78:22010}$-C_2	2	0.0	1.40	310.9
$C_{78:81138}^{1h}$-C_s	2	14.3	0.76	294.7	$C_{78:83318}^{1h}$-C_s	2	1.8	0.76	297.6	$C_{78:185809}^{1h}$-C_s	2	9.0	0.88	310.4
$C_{78:22010}$-C_2	2	18.6	1.29	304.5	$C_{78:185809}^{1h}$-C_s	2	5.4	0.77	316.9	$C_{78:21975}$-C_1	2	9.5	1.33	294.7
$C_{78:185809}^{1h}$-C_s	2	18.9	0.71	312.9	$C_{78:185820}^{1h}$-C_s	2	6.5	0.93	315.1	$C_{78:83318}^{1h}$-C_s	2	10.7	0.76	285.8
$C_{78:185820}^{1h}$-C_s	2	21.8	0.88	309.2	$C_{78:24088}$-C_{2v}	2	10.8	0.93	299.0	$C_{78:185820}^{1h}$-C_s	2	10.8	0.98	308.1
$C_{78:185895}^{1h}$-C_1	2	26.1	0.85	300.0	$C_{78:21975}$-C_1	2	12.0	1.24	295.0	$C_{78:22646}$-C_1	2	10.9	1.18	289.4
$C_{78:24088}$-C_{2v}	2	28.4	0.89	290.9	$C_{78:22646}$-C_1	2	12.3	1.15	290.9	$C_{78:24088}$-C_{2v}	2	15.4	0.93	291.7
$C_{78:83321}^{1h}$-C_1	2	28.9	0.84	274.5	$C_{78:185895}^{1h}$-C_1	2	12.5	0.93	304.3	$C_{78:21981}$-C_1	2	16.9	0.97	299.0
$C_{78:24107}$-C_{2v}	0	29.3	0.73	234.4	$C_{78:24109}$-D_{3h}	0	13.9	1.09	243.8	$C_{78:185895}^{1h}$-C_1	2	17.6	0.98	296.5
$C_{78:185814}^{1h}$-C_1	2	31.2	0.49	276.2	$C_{78:83321}^{1h}$-C_1	2	14.4	0.81	279.5	$C_{78:185827}^{1h}$-C_1	2	20.1	0.34	272.0
$C_{80:31924}$-I_h	0	0.0	1.49	311.7	$C_{80:31924}$-I_h	0	0.0	1.53	314.7	$C_{80:31924}$-I_h	0	0.0	1.45	305.5
$C_{80:31923}$-D_{5h}	0	16.6	1.27	283.9	$C_{80:31923}$-D_{5h}	0	15.2	1.34	288.2	$C_{80:112912}^{1h}$-C_s	2	7.6	1.16	322.9
$C_{80:112912}^{1h}$-C_s	2	26.8	1.08	310.1	$C_{80:112912}^{1h}$-C_s	2	15.2	1.16	324.5	$C_{80:31923}$-D_{5h}	0	14.6	1.30	279.9
$C_{80:31922}$-C_{2v}	0	36.5	0.55	264.6	$C_{80:112913}^{1h}$-C_1	2	29.0	0.86	304.3	$C_{80:112913}^{1h}$-C_1	2	20.9	0.82	303.2
$C_{80:112913}^{1h}$-C_1	2	37.6	0.88	292.7	$C_{80:248984}^{1h}$-C_1	2	29.5	0.76	305.5	$C_{80:248984}^{1h}$-C_1	2	22.1	0.72	303.7
$C_{80:248984}^{1h}$-C_1	2	38.2	0.77	293.9	$C_{80:31922}$-C_{2v}	2	36.3	0.63	267.5	$C_{80:31922}$-C_{2v}	0	32.4	0.63	262.5
$C_{82:39718}$-C_{2v}	0	0.0	0.79	272.7	$C_{82:39718}$-C_{2v}	0	0.0	0.89	277.2	$C_{82:39705}$-C_{2v}	1	0.0	1.27	312.7
$C_{82:39705}$-C_{2v}	1	5.5	1.17	301.7	$C_{82:39705}$-C_{2v}	1	0.3	1.27	311.5	$C_{82:39718}$-C_{2v}	0	1.2	0.95	277.1
$C_{82:39663}$-C_s	1	5.6	1.47	294.6	$C_{82:39663}$-C_s	1	3.5	1.51	301.5	$C_{82:332127}^{1h}$-C_1	2	2.4	0.76	316.8
$C_{82:39715}$-C_s	0	12.9	0.59	258.9	$C_{82:332127}^{1h}$-C_1	2	9.5	0.75	308.6	$C_{82:39714}$-C_2	0	11.2	0.64	262.9
$C_{82:39717}$-C_{3v}	0	17.1	0.27	266.0	$C_{82:39715}$-C_s	0	10.2	0.55	266.4	$C_{82:39663}$-C_s	1	11.3	1.44	294.9
$C_{82:332127}^{1h}$-C_1	2	20.3	0.82	293.4	$C_{82:39717}$-C_{3v}	0	11.1	0.39	276.8	$C_{82:39717}$-C_{3v}	0	12.6	0.28	276.2
$C_{82:39714}$-C_2	0	22.3	0.65	246.4	$C_{82:39714}$-C_2	0	26.2	0.71	247.1	$C_{82:39715}$-C_s	0	14.1	0.53	263.6

In labelling the cages, we refer to classical fullerene isomers by their positions in the sequence of canonical spirals. To distinguish the non-classical isomers we use an extra superscript (1h) and use positions in the sequence of canonical spirals for the single-heptagon isomers. To avoid ambiguity, we list canonical spirals explicitly for these structures in the supporting information (S2). [The spiral is a sequence of 5s and 6s (and in this case also 7s) representing a helical strip of faces which can be wound up to reconstruct the surface of the 3D cage, in the manner of 'unpeeling' an orange; if the list is interpreted as an integer with one digit for each face, the canonical spiral for a given isomer is the one that gives the lowest such number; it is specified by the positions of non-hexagonal faces in the sequence (hence by 12 numbers for a classical fullerene and 14 for a non-classical fullerene with one heptagonal face)].

Results and Discussion

$Sc_3N@C_{78}$ is based on the D_{3h}-symmetric classical fullerene $C_{78}:24109$ ($C_{78}:5$ in the IPR-only sequence) and this TNT-EMF has a large HOMO-LUMO gap (1.23eV), in agreement with experimental and other theoretical results [30, 31]. The isomer with the second low energy has a non-classical cage ($C_{78}^{1h}:83318$) with two pairs of fused pentagons, lies 14.3 kcal mol⁻¹ above the first, and has a much smaller HOMO-LUMO gap (0.76 eV). In fact, the ten lowest-energy isomers (Table 1) include six non-classical cages, but with energies that preclude significant thermal population.

For YSc$_2$N@C$_{78}$, on the other hand, the isomer with the lowest energy also has a large HOMO-LUMO gap (1.37eV) and is a classical, but non-IPR cage, C$_{78}$:22010 with two pentagon adjacencies. The same cage has been reported as the parent in Gd$_3$N@C$_{78}$ [13, 32], Y$_3$N@C$_{78}$ [13b, 33], and GdSc$_2$@C$_{78}$ [13c]; in these cases, as for YSc$_2$N, the central TN is larger than Sc$_3$N. The isomer with the second lowest energy is non-classical but lies only 1.8 kcal mol^{-1} higher, so could be expected to have significant population in an equilibrium mixture at 1000K. LaSc$_2$N@C$_{78}$ is predicted to have the same most favored cage as YSc$_2$@C$_{78}$, but a second isomer based on a (different) non-classical cage (C$_{78}^{1h}$:185809) that also has two pentagon adjacencies, and lies 9.0 kcal mol^{-1} above the best classical isomer.

Our calculations find icosahedral C$_{80}$:31924 (C$_{80}$:7 in the IPR-only sequence) to be the best cage for all three cases MSc$_2$ with M=Sc, Y and La. There is competition for the second place in the energy order between a classical IPR parent of maximum symmetry D$_{5h}$ (C$_{80}$:31923) and a one-heptagon non-classical isomer (C$_{80}^{1h}$:112912). For Sc$_3$N, both cages lie well above the best candidate, with the non-classical cage lagging behind the second best classical cage; for YSc$_2$N, the two competing isomers have essentially equal energy, and for LaSc$_2$N, the isomer with the non-classical parent cage has edged into second place. This non-classical isomer of LaSc$_2$N@C$_{80}$ has a gap of 1.16eV (compared with the gaps of the best isomers of MSc$_2$N@C$_{80}$ of 1.49, 1.53 and 1.45eV for M=Sc, Y and La, respectively). Gratifyingly, the three isomers of LaSc$_2$N@C$_{80}$ predicted in our systematic calculations to have lowest energy match those reported as experimental isomers by Zhang et al. [25a], who give a crystal structure for a non-classical isomer based on cage C$_{80}^{1h}$:112912. Their calculations based on the cages found in the three experimental structures also agree with our energy order.

In terms of the calculated relative energy of its hexa-anion (S3), C$_{82}$:39718 (C$_{82}$:9 in the IPR-only sequence) is the best candidate cage for encapsulating a TN cluster, and indeed the calculations show that Sc$_3$N@C$_{82}$:39718 is the isomer with the lowest energy

within the set for Sc$_3$N@C$_{82}$, despite the low calculated HOMO-LUMO gap (0.79 eV). A recent experimental report finds the same cage structure for Sc$_3$N@C$_{82}$ [34]. It is interesting to note that the five most favored isomers of Sc$_3$N@C$_{82}$ in our calculations coincide with the first five favored isomers predicted by Popov et al. [35], with minor variations in order. For YSc$_2$N@C$_{82}$ and LaSc$_2$N@C$_{82}$, the same non-IPR cage (C$_{82}$:39705) is found in the TNT-EMF structures of lowest energy, in both cases with a HOMO-LUMO gap comparable to those of already synthesized TNT-EMFs.

It should be noted that the predicted cages and geometrical parameters for the lowest-energy isomers of MSc$_2$N@C$_n$ calculated here are also in good agreement with available experimental data (see S4). Thus the employed method is reliable.

The fact that TNT-EMFs based on non-classical cages are predicted in several cases to be competitive with those based on classical cages is a resultant of a complex set of factors. Non-classical cages including one heptagonal face tend to have more pentagon adjacencies (almost universally [36] destabilizing in the neutral, although offset by the favorable effect of pentagon-heptagon adjacencies [37, 38]), but these offer potential electron-acceptor sites (stabilizing in an anion). The encapsulated TN cluster is generally accepted to act as a formal six-electron donor [4, 39]. Loss of electrons appears to accentuate bond-length differences in mixed clusters, as for example in free MSc$_2$N (M=Y and La) where the M-N distances shrink but Sc-N distances increase in the positive ions. One-heptagon cages also have naturally low symmetry (at best C$_s$ or C$_1$), which may enhance their geometric match with mixed TN clusters, in analogy to classical TNT-EMFs such as DySc$_2$N@C$_{76}$, where the cluster is encapsulated in C$_s$-symmetric C$_{76}$:17490, instead of T$_d$ C$_{76}$:19151, even though the hexa-anion of the latter (more symmetrical) cage is lower in energy by 20.8 kcal mol^{-1} [15].

The calculations reported here give a set of favored structures for TNT-EMFs with three different clusters MSc$_2$N embedded in C$_n$ cages of three different nuclearities. As discussed above, the identification of

lowest energy isomers is in agreement with available data [30, 34, 39, 40]; the results include cases where the optimal cage is the same for M=Sc, Y, La, e.g. C_{80}:31924, and others where the optimal cage depends on M (C_{78}:24109 for M=Sc, but C_{78}:22010 for M=Y, La). The cages, both classical and non-classical, that occur in the low-energy sets exhibit a complex network of connections, as large parts of the structures are conserved for given cage size and between cage sizes. Fig. 2 illustrates some of these connections for cages involved in low-energy isomers of $Sc_3N@C_n$ (n = 78, 80 and 82). The illustrated isomers are the five lowest energy for n = 78 and 82, but for n = 80 the isomers of lowest energy have been supplemented with a cage (C_{80}:31891) that is actually seventh in energy order.
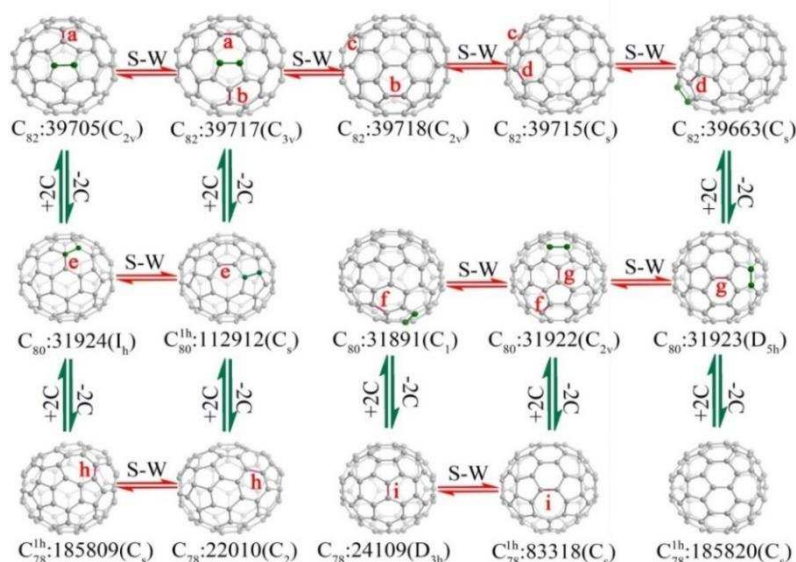

Fig. 2 Structural connections among TNT-EMFs. The pairs of letters in red indicate that a Stone-Wales isomerization transformation is taking place for the two corresponding bonds; the pairs of atoms in C_n marked in green indicate that those atoms come from a C_2 unit added by an Endo-Kroto insertion into the indicated C_{n-2} cage. The correspondence between general-isomer and IPR-isomer nomenclature for isolated-pentagon cages is: C_{78}:24109 (IPR: 5), C_{78}:24107 (IPR: 3), C_{80}:31924 (IPR: 7), C_{80}:31923 (IPR: 6), C_{80}:31922 (IPR: 5), C_{82}:39718 (IPR: 9), C_{82}:39715 (IPR: 6), C_{82}:39717 (IPR: 8).
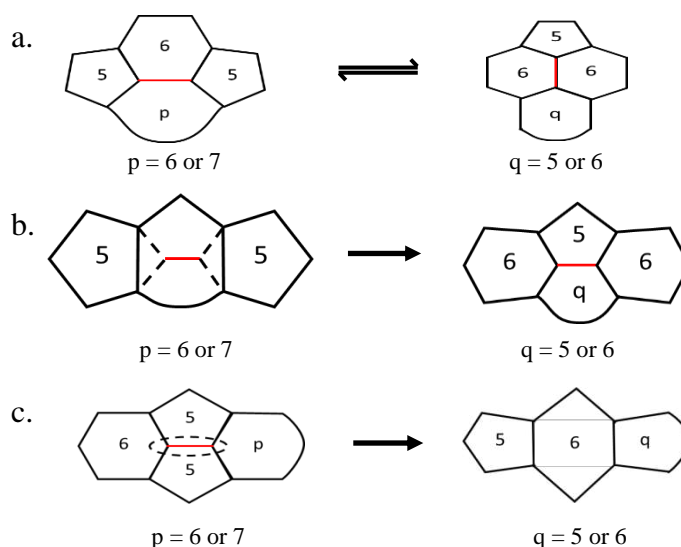

Fig.3 Transformations used to connect the fullerene cages of low-energy TNT-EMF isomers. a) Generalized Stone-Wales isomerization; b) Endo-Kroto Insertion of C_2; c) C_2 extrusion.

5

The figure shows connections through processes of two types: Stone-Wales (S-W) isomerization [41, 42], and expansion/contraction via Endo-Kroto (E-K) C_2 insertion/extrusion [43], in each case generalized to allow one face of the transforming patch to be either a hexagon or heptagon (see Figure 3 for details).

The map is not intended to be exhaustive, in that the isomers shown also connect many isomers outside the set and up and down to nuclearities 84 and 76, but it does illustrate the high degree of commonality between cages that have featured in experimental observations of TNT-EMFs.

Exploring the rows of the map first: for n = 78, both the parent cage of $Sc_3N@C_{78}$ (C_{78}:24109) and the parent of C_{78}-based TNT-EMFs with encapsulated YSc_2N, $LaSc_2N$, Y_3N and Gd_3N (C_{78}:22010) are a single S-W step away from a one-heptagon cage of low energy.

In the row of C_{80} cages, the well-known icosahedral isomer (C_{80}:31924, i.e. C_{80}:7 in the IPR-only sequence), the cage for the lowest energy isomer of many EMFs [44-50], is connected by a single S-W step to the recently identified non-classical one-heptagonal isomer (C_{80}^{1h}:112912). A single S-W step from C_{80}:31923, the IPR parent cage of the second most stable isomer of $Sc_3N@C_{80}$ and parent cage for many EMFs [51-55], recovers the fourth most stable isomer $Sc_3N@C_{80}$ and another S-W step gives a non-IPR cage that links by E-K C_2 loss to the D_{3h} isomer that is favored by a number of EMFs with C_{78} cages [56-59].

The C_{82} row again includes cages that have featured heavily in both experimental and theoretical structures of TNT-EMFs and often EMFs. At the left of the row, cage C_{82}:39705 is favored for Y_3N encapsulation [35]. The isomer in the center of the S-W chain (C_{82}:39718) is common to many mono-metallic EMFs; for example, it can encapsulate most of the lanthanides [1]. The cage at the right of the S-W chain (C_{82}:39663) is the parent cage of $Y_3N@C_{82}$ [60]. C_{82}:39717 is the parent of $Sc_2S@C_{82}$ and $Sc_2C_2@C_{82}$ [61], and C_{82}:39715 is the parent of $Sc_2C_2@C_{82}$, $Y_2C_2@C_{82}$[62], in all of which the fullerene cage is acting as a formal acceptor of only four electrons.

Vertical connections in the map are made by C_2 insertion and extrusion, which provides a route for expansion of all five parents of low-energy isomers of $Sc_3N@C_{78}$ into the isomers of $Sc_3N@C_{80}$ with relatively low energy, and the most favored isomers for $Sc_3N@C_{80}$ are again connected to the favored isomers of $Sc_3N@C_{82}$. It is worth noting that two non-classical one-heptagon parent cages for C_{78}, and one for C_{80}, lie on direct paths between low-energy classical isomers of $Sc_3N@C_n$ and $Sc_3N@C_{n+2}$. Further connections can be made to species that lie outside this small region of the full inter-conversion map. For example, C_2 addition to C_{82}:39718 can form C_{84}:51365, the parent cage of $Tb_3N@C_{84}$ [18] and $Tm_3N@C_{84}$ [19]. Likewise, removal of C_2 from the parent cage of $YSc_2N@C_{78}$ and $LaSc_2N@C_{78}$ (C_{78}:22010) can yield C_{76}:17490, the parent cage of $YSc_2N@C_{76}$, $DySc_2N@C_{76}$ [15], and the isomer of $Sc_3N@C_{76}$ with the second lowest predicted energy.

Thus, at least in a formal sense, the parent fullerene cages and hence the low-energy TNT-EMFs based on them, can be transformed one into another. These structural relationships express a tendency of favored cages to be built from common stabilizing substructures and motifs. Moreover, the close correspondence of calculated structures with experiment and with each other suggests that theory has a powerful role to play in rationalizing observations and predicting new possibilities, given that the soot produced by the arc-discharge method is often a complex mixture [19, 25] with yields that correlate with overall energy.

Our calculations demonstrate C_2 insertion/extrusion is not only a topological but also an energetic bridge for growth/degradation of favored TNT EMFs. Previous theoretical studies have shown that C_2 insertion can facilitate the formation of favored fullerenes/EMFs smaller than C_{60}/C_{50} [63]. To our knowledge, there is no evidence that the formation mechanisms of small fullerenes differ dramatically from those of medium-sized fullerenes; C_2 insertion could also facilitate the formation of fullerenes with sizes larger than C_{60}. Since the most common parent cages of EMFs, i.e. D_{3h}-C_{78}, I_h-C_{80} and C_{2V}-C_{82} are all IPR-satisfying, they cannot be formed by direct C_2

insertion into classical fullerene isomers, without the help of an isomerization (for which S-W transformation is the best candidate). If, however, a heptagon is available in a carbon cage C_n, an IPR-satisfying cage of C_{n+2} can be formed directly via C_2 insertion into the heptagon, as in the cases of I_h-C_{60} and I_h-C_{80} discussed below; even then, S-W isomerization is needed for transformations between heptagon-including isomers and classical isomers of C_n. S-W isomerization and E-K C_2 insertion/extrusion are complementary steps in the simplest picture for the formation of EMFs.

The role of non-classical isomers in empty fullerene growth has been modeled [64], and one-heptagon isomers have been proposed to contribute to the high relative abundance of I_h-symmetrical C_{60}, since this isomer can be formed by C_2 insertion into the most stable one-heptagon isomer of C_{58} [64]. Theoretical study showed that non-classical isomers of C_{68} containing a heptagon play a key role in the formation of fullerene C_{70} and fullerene derivative $C_{68}Cl_6$ [65]. In the map shown in Figure 2, the cage C_{80}:31924, the parent of many EMFs, is similarly related by C_2 insertion to the one-heptagon isomer C_{78}^{1h}:185809. It seems reasonable to ascribe at least part of the abundance of I_h-C_{80}-based EMFs to a similar mechanism. I_h-C_{80} cage also has other pathways from C_{82}, as it is related to C_{82}:39705 by E-K C_2 extrusion and to the favored non-classical cage C_{80}^{1h}:112912 by S-W isomerization. Given also the special stability of its hexa-anion of I_h-C_{80} [39], it is plausible that I_h-C_{80}-based TNT-EMFs should dominate yields. These considerations show that a heptagon play an important role for the formation of favored EMFs.

The map given in Figure 2 can be read as a scheme for either growth or degradation of TNT-EMFs. In fact, quantum molecular dynamics simulations show that hot giant fullerenes can both lose and gain carbon in high-temperature conditions [66], which is compatible with our theoretical findings that EMFs can grow or degrade into other sized species and form a structural web of favored EMFs together with the help of S-W isomerization.

One indicator of the thermodynamic driving force for reactions that lead to formation of a TNT-EMF is the encapsulation energy, E_{en}, which is the difference in energy between reactants and product. Since the discussions below are based on clusters of similar geometrical shape encapsulated in a given cage isomer, the basis set superposition errors (BSSE) for different reactions are expected to be comparable. To check this, we include counterpoise corrections in the calculation of E_{en}. The calculations confirm that the BSSEs are comparable, and lead to corrected encapsulation energies of Sc_3N, YSc_2N and $LaSc_2N$ in C_{78}:24109 of 267.3, 243.8 and 226.2 kcal mol^{-1}, respectively. Evidently, C_{78}:24109 is a tight fit for the YSc_2N cluster and unsuitable for encapsulating the $LaSc_2N$ cluster. The encapsulation energies of the three clusters for C_{78}:22010 are 304.5, 313.7 and 310.9 kcal mol^{-1}, respectively; they suggest that this cage is suitable for YSc_2N and $LaSc_2N$ clusters. The encapsulation energies inside C_{80}:31924 of 311.7, 314.7 and 305.5 kcal mol^{-1}, suggesting a slight preference for this cage as encapsulant for the first two clusters. For the same clusters in C_{80}:31923 the energies are 283.9, 288.2 and 279.9 kcal mol^{-1}, suggesting that this cage is less favored for $LaSc_2N$. However, one-heptagon C_{80}^{1h}:112912 with E_{en} = 322.9 kcal mol^{-1} is readier to encapsulate $LaSc_2N$ than C_{80}:31923, in agreement with the experimental observation that one-heptagon $LaSc_2N@C_{80}^{1h}$:112912 has been isolated and characterized [25a], even though its parent cage is easily to transform into other favored cages of TNT-EMFs. The encapsulation energies of the three clusters inside C_{82}:39705 are 301.7, 311.5 and 312.7 kcal mol^{-1}, suggesting that C_{82}:39705 is more suitable for containing YSc_2N and $LaSc_2N$ clusters.

Finally, a remark can be made on selection of candidate cages. Recently, Yamada et al. revisited the structure of $Sc_2@C_{66}$, and found two scandium atoms located inside a C_{2V} cage, C_{68}:4059, with four pentagon adjacencies in two well-separated pairs, each associated with one scandium atom [67]. The larger cages considered in the present study of TNT-EMFs encapsulate molecular clusters. The fact that all low-energy isomers found have two or fewer

adjacencies (Table 1) is retrospective justification of the three-adjacency limit applied for classical cages.

Conclusion

In summary, the regimes of classical and non-classical fullerene cages can be bridged via S-W isomerization and C_2 insertion/extrusion. Extensive density functional theory calculations demonstrate that there is a dense network of structural interconnections between the favored isomers of TNT-EMFs of C_{78}, C_{80} and C_{82}, and that one-heptagon non-classical TNT-EMFs are close to classical TNT-EMFs in terms of total energetics. In particular, species such as classical $MSc_2N@C_{78}$:22010 (M=Y and La), $YSc_2N@C_{80}$:31924 and $MSc_2N@C_{82}$:39705 (M=Y and La), and non-classical $YSc_2N@C_{78}^{1h}$:83318 are promising candidates for synthesis of new TNT-EMFs. The existence of the network of insertion/extrusion and S-W isomerization between lowest-energy isomers suggests a route for formation of TNT-EMFs, in which non-classical one-heptagon cages may play a significant role.

Acknowledgements

References

[1] a) H. Shinohara, Rep. Prog. Phys. **2000,** 63, 843. b) A. Rodríguez-Fortea, A. L. Balch, J. M. Poblet, Chem. Soc. Rev. **2011,** 40, 3551.

[2] Y. Chai, T. Guo, C. Jin, R. E. Haufler, L. P. F. Chibante, J. Fure, L. Wang, J. M. Alford, R。 E。 Smalley, J. Phys. Chem. **1991,** 95, 7564.

[3] T. Akasaka, S. Nagase, Endofullerenes: A New Family of Carbon Clusters, Kluwer Academic, Dordrecht, 2002.

[4] A. A. Popov, S. Yang, Chem. Rev. **2013,** 113, 5989.

[5] a) L. Dunsch, S. Yang, Small **2007,** 3, 1298. b) J. Zhang, S. Stevenson, H. C. Dorn, Acc. Chem. Res. **2013,** 46, 1548.

[6] H. W. Kroto, Nature **1987,** 329, 529.

[7] M. Takata, B. Umeda, E. Nishibori, M. Sakata, Y. Saito, M. Ohno, Nature **1995,** 377, 46.

[8] K. Kobayashi, S. Nagase, J. Am. Chem. Soc. **1997,** 119, 12693.

[9] P. W. Fowler, D. E. Manolopoulos, Nature **1992**, 355, 428.

[10] C. R. Wang, T. Kai, T. Tomiyama, T. Yoshida, Y. Kobayashi, E. Nishibori, M. Takata, M. Sakata, H. Shinohara, Nature **2000,** 408, 426. b) S. Stevenson, P. W. Fowler, T. Heine, J. C. Duchamp, G. Glass, T. Rice, K. Harich, E. Hajdu, R. Bible, H. C. Dorn, Nature **2000,** 408, 427.

[11] a) S. F. Yang, A. A. Popov, L. Dunsch, Angew. Chem. Int. Ed. **2007,** 46, 1256. b)N. Chen, M. Mulet-Gas, Y. Y. Li, R. E. Stene, C. W. Atherton, A. Rodríguez-Fortea, J. M. Poblet, L. Echegoyen, Chem. Sci. **2013,** 4, 180. c) N. Chen, C. M.Beavers, M. Mulet-Gas, A. Rodríguez-Fortea, E. J. Munoz, Y. -Y. Li, M. M. Olmstead, A. L. Balch, J. M. Poblet, L. Echegoyen, J. Am. Chem. Soc. **2012,** 134, 7851.

[12] H. Kato, A. Taninaka, T. Sugai, H. Shinohara. J. Am. Chem. Soc. **2003,** 125, 7782.

[13] a) C. M. Beavers, M. N. Chaur, M. M. Olmstead, L. Echegoyen, A. L. Balch, J. Am. Chem. Soc. **2009,** 131, 11519. b) J. Zhang, D. W. Bearden, T. Fuhrer, L. Xu, W. Fu, T. Zuo, H. C. Dorn. J. Am. Chem. Soc. **2013**, 135, 3351. c) A. L. Svitova, A. A. Popov, and L. Dunsch, Inorg. Chem. **2013,** 52, 3368.

[14] B. Q. Mercado, C. M. Beavers, M. M. Olmstead, M. N. Chaur, K. Walker, B. C.Holloway, L. Echegoyen, A. L. Balch. J. Am. Chem. Soc. **2008,** 130, 7854.

[15] S. Yang, A. A. Popov, L. Dunsch, J. Phys. Chem. B **2007,** 111, 13659.

[16] X. Lu, H. Nikawa, T. Nakahodo, T. Tsuchiya, M. O. Ishitsuka, Y. Maeda, T. Akasaka, M. Toki, H. Sawa, Z. Slanina, N. Mizorogi, S. Nagase, J. Am. Chem. Soc. **2008,** 130, 9129.

[17] Z. Q. Shi, X. Wu, C. R. Wang, X. Lu, H. Shinohara, Angew. Chem. Int. Ed. **2006,** 118, 2161.

[18] C. M. Beavers, T Zuo, J. C. Duchamp, K. Harich, H. C. Dorn, M. M. Olmstead, A. L. Balch. J. Am. Chem. Soc. **2006,** 128, 11352.

[19] T. Zuo, K. Walker, M. M. Olmstead, F. Melin, C. B Holloway, L. Echegoyen, H. C. Dorn, M. N. Chaur, C. J. Chancellor, C. M. Beavers, A. L. Balch, A . Athans. J. Chem. Commun. **2008,** 1067.

[20] P. A. Troshin, A. G.Avent, A. D. Darwish, N. Martsinovich, A. K. Abdul-Sada, J. M.Street, R. Taylor. Science **2005,** 309, 278.

[21] I. N. Ioffe, C. Chen, S. Yang, L. N. Sidorov, E. Kemnitz, S. I. Troyanov, Angew. Chem. Int. Ed. **2010,** 49, 4784.

[22] I. N. Ioffe, O. N. Mazaleva, L. N. Sidorov, S. Yang, T. Wei, E. Kemnitz, S. I. Troyanov, Inorg. Chem. **2013,** 52, 13821.

[23] a) S. Yang, S. Wang, E. Kemnitz, and S. I. Troyanov, Angew. Chem. Int. Ed. **2014,** 53, 2460; b) S. Yang, T. Wei, K.

Scheurell, E. Kemnitz, and S. I. Troyanov, Chem. Eur. J. **2015,** 21, 15138 c) T. Wei, S. Yang, E. Kemnitz, and I. S. Troyanov . Chem. Asian J. **2015,** 10, 559.

[24] Z. Y. Tan, T. R. Chen, Z. J. Liao, J. Li, F. Zhu, X. Lu, S. Y. Xie, J. Li, R. B. Huang, L. S. Zheng. Nature Comm. **2011,** 1.

[25] a) Y. Zhang, K. B. Ghiassi, Q. Deng, N. A. Samoylova, M. M. Olmstead, A. L. Balch, A. A. Popov. Angew. Chem. Int. Ed. **2015,** 54, 495; b) S. Stevenson, C. B. Rose, J. S. Maslenikova, J. R. Villarreal, M. A. Mackey, B. Q. Mercado, K. Chen, M. M. Olmstead, and A. L. Balch . Inorg. Chem. **2012,** 51, 13096.

[26] P. W. Fowler. D. E.Manolopoulos, An Atlas of Fullerenes Clarendon Press, Oxford, 1995.

[27] D. E. Manolopoulos and P. W. Fowler, J. Chem. Phys. **1992**, 96, 7603.

[28] M. J. Frisch, Gaussian 09, Revision A. 02 Gaussian Inc.: Pittsburgh, PA, 2009.

[29] a) B. Delley, J. Chem. Phys. **1990**, 92, 508 b) B. Delley. J. Chem. Phys. **2000**, 113, 7756 c) J. P. Perdew and Y. Wang, Phy. Rev. B **1992**, 45, 13244.

[30] M. M. Olmstead, A. Bettencourt-Dias, J. C. Duchamp, S. Stevenson, D. Marciu, H. C. Dorn, A. L. Balch. Angew. Chem. Int. Ed. **2001,** 40, 1223.

[31] A. A. Popov, M. Krause, S. Yang, J. Wong, L.Dunsch, J. Phys. Chem. B **2007,** 111, 3363.

[32] T. Yang, X. Zhao, S. L. Li, J. -J. Zheng, W. -Y. Gao, ChemPhysChem, **2012,** 13, 449.

[33] Y. Ma, T. Wang, J. Wu, Y. Feng, W. Xu, L. Jiang, J. Zheng, C. Shu, C. Wang. Nanoscale **2011** 3, 4955.

[34] T. Wei, S. Wang, F. Liu, Y. Tan, X. Zhu, S. Xie, S. Yang, J. Am. Chem. Soc. **2015,** 137, 3119.

[35] A. A. Popov, L. Dunsch, J. Am. Chem. Soc. **2007,** 129, 11835.

[36] A. S. Matias, R. W. A. Havenith, M. Alcami, A. Ceulemans, Phys Chem Chem Phys **2016** DI: 10. 1039/c5cp04970a

[37] L. -H. Gan, J. -Q. Zhao, Q. Hui, J. Comput. Chem. **2010,** 31, 1715.

[38] a) P. W. Fowler, T. Heine, D. Mitchell, G. Orlandi, R. Schmidt, G. Seifert, F. Zerbetto, J. Chem. Soc. , Faraday Trans. **1996,** 92, 2203. b) A. Ayuela, P. W. Fowler, D. Mitchell, R. Schmidt, G. Seifert, F. Zerbetto, J. Phys. Chem. **1996,** 100, 15634.

[39] J. M. Campanera, C. Bo, J. M. Poblet, Angew. Chem. Int. Ed. **2005,** 44, 7396.

[40] H. M. Lee, M. M. Olmstead, E. Iezzi, J. C. Duchamp, H. C. Dorn, A. L. Balch, J. Am. Chem. Soc. **2002,** 124, 3494.

[41] B. R. Eggen, M. I. Heggie, G. Jungnickel, C. D. Latham, R. Jones, P. R. Briddon. Science **1996**, 272, 87.

[42] Bettinger, H. F. Yakobson, B. I. Scuseria, G. E. J. Am. Chem. Soc. **2003,** 125, 5572.

[43] M. Endo, H. W. Kroto, J. Phys. Chem. **1992,** 96, 6941.

[44] S. Stevenson, G. Rice, T. Glass, K. Harich, F. Cromer, M. R. ordan, J. Craft, E. Hadju, R. Bible, M. M. Olmstead, K. Maitra, A. J. Fisher, A. L. Balch, H. C. Dorn, Nature **1999,** 401, 55.

[45] S. Yang, L. Dunsch, Chem. Eur. J. **2006,** 12, 413.

[46] M. N. Chaur, F. Melin, B. Elliott, A. J. Athans, K. Walker, B. C. Holloway, L. Echegoyen, J. Am. Chem. Soc. **2007,** 129, 14826.

[47] E. B. Iezzi, J. C. Duchamp, K. R. Fletcher, T. E. Glass, H. C. Dorn, Nano Lett. **2002,** 2, 1187.

[48] S. Stevenson, M. A. Mackey, M. A. Stuart, J. P. Phillips, M. L. Easterling, C. J. Chancellor, M. M. Olmstead, A. L. Balch, J. Am. Chem. Soc. **2008,** 130, 11844.

[49] a) T. -S. Wang, N. Chen, J. -F. Xiang, B. Li, J. -Y. Wu, W. Xu, L. Jiang, K. Tan, C. -Y. Shu, X. Lu, C. -R. Wang, J. Am. Chem. Soc. **2009,** 131, 16646；b) T. -S. Wang, C. -R. Wang Acc. Chem. Res. **2014,** 47, 450.

[50] a) Y. Iiduka, T. Wakahara, T. Nakahodo, T. Tsuchiya, A. Sakuraba, Y. Maeda, T. Akasaka, K. Yoza, E. Horn, T. Kato, M. T. H. Liu, N. Mizorogi, K. Kobayashi, S. Nagase, J. Am. Chem. Soc. **2005,** 127, 12500.

[51] T. Zuo, C. M. Beavers, J. C. Duchamp, A. Campbell, H. C. Dorn, M. M. Olmstead, A. L. Balch, J. Am. Chem. Soc. **2007,** 129, 2035.

[52] M. Yamada, N. Mizorogi, T. Tsuchiya, T. Akasaka, S. Nagase, Chem. Eur. J. **2009,** 15, 9486.

[53] T. Zuo, M. M. Olmstead, C. M. Beavers, A. L. Balch, G. Wang, G. T. Yee, C. Shu, L. Xu, B. Elliot, L. Echegoyen, J. C. Duchamp, H. C. Dorn, Inorg. Chem. **2008,** 47, 5234.

[54] A) M. Krause, L. Dunsch, ChemPhysChem. **2004,** 5, 1445. b) S. F. Yang, L. Dunsch Chem. Eur. J. **2006,** 12, 413.

[55] a) M. Krause, J. Wong, L. Dunsch, Chem. Eur. J. **2005,** 11, 706. b) S. Stevenson, M. A. Mackey, C. E. Coumbe, J. P. Phillips, B. Elliott, L. Echegoyen, J. Am. Chem. Soc. **2007,** 129, 6072.

[56] B. P. Cao, T. Wakahara, T. Tsuchiya, M. Kondo, Y. Maeda, G. M. A. Rahman, T. Akasaka, K. Kobayashi, S. Nagase, K. Yamamoto, J. Am. Chem. Soc. **2004,** 126, 9164.

[57] B. Cao, H. Nikawa, T. Nakahodo, T. Tsuchiya, Y. Maeda, T.

Akasaka, H. Sawa, Z. Slanina, N. Mizorogi, S. Nagase, J. Am. Chem. Soc. **2008,** 130, 983.

[58] a) M. Yamada, T. Wakahara, T. Tsuchiya, Y. Maeda, M. Kako, T. Akasaka, K. Yoza, E. Horn, N. Mizorogi, S. Nagase, Chem. Commun. **2008,** 558-560. b) K. Tan, X. Lu, Chem. Commun. **2005,** 4444.

[59] T. Yumura, Y. Sato, K. Suenaga, S. Iijima, J. Phys. Chem. B **2005,** 109, 20251.

[60] W. Fu, L. Xu, H. Azurmendi, J. Ge, T. Fuhrer, T. Zuo, J. Reid, C. Shu, K. Harich, H. C. Dorn, J. Am. Chem. Soc. **2009,** 131, 11762.

[61] a) L. Dunsch, S. F. Yang, L. Zhang, A. Svitova, S. Oswald, A. A. Popov, J. Am. Chem. Soc. **2010,** 132, 5413. b) Y. Iiduka, T. Wakahara, K. Nakajima, T. Nakahodo, T. Tsuchiya, Y. Maeda, T. Akasaka, K. Yoza, M. T. H. Liu, N. Mizorogi, S. Nagase, Angew. Chem. Int. Ed. **2007,** 46, 5562.

[62] X. Lu, K. Nakajima, Y. Iiduka, H. Nikawa, N. Mizorogi, Z. Slanina, T. Tsuchiya, S. Nagase, Akasaka, T. J. Am. Chem. Soc. **2011,** 133, 19553.

[63] J. -S. Dang, W. -W. Wang, J. -J. Zheng, X. Zhao, E. Ōsawa, Nagase, S. J. Phys. Chem. C **2012**, 116, 16233. b) M. Mulet-Gas, L. Abella, P. W. Dunk, A. Rodr´ıguez-Fortea, H.W. Kroto and J. M. Poblet，Chem. Sci., **2015**, 6, 675.

[64] E. Hernández, P. Ordejón, H. Terrones, Phys. Rev. B **2001,** 63, 193403.

[65] W.-W. Wang, J.-S. Dang, J.-J. Zheng, and X. Zhao, J. Phys. Chem. C 2012, 116, 17288.

[66] B. Saha, S. Irle, K. Morokuma, J. Phys. Chem. C **2011**, 115, 22707.

[67] M. Yamada, H. Kurihara, M. Suzuki, J. Dong Guo, M. Waelchli, M. M. Olmstead, A. L. Balch, S. Nagase, Y. Maeda, T. Hasegawa, X. Lu, and T. Akasaka, J. Am. Chem. Soc. 2014, 136, 7611.